Sādhanā Vol. 28, Parts 1 & 2, February/April 2003, pp. 63–80. © Printed in India

Melting behaviour of lead and bismuth nano-particles in quasicrystalline matrix - The role of interfaces

ALOK SINGH[1]* and A P TSAI[2]

[1]Physical Metallurgy Section, Materials Characterisation Group, Indira Gandhi Centre for Atomic Research, Kalpakkam 603 102, India
[2](*Present address) National Institute for Materials Science, 1-2-1 Sengen, Tsukuba 305-0047, Japan
e-mail: alok@quasi.nims.go.jp

Abstract. Nanomaterials are playing an increasingly important role in modern technologies. Interfaces are crucial in nanotechnology. In this study, we have examined the stability of nanoparticles. Major emphasis is on understanding the effect of interfaces on melting. Melting behaviour of nanocrystalline interfaces, created by embedding lead and bismuth nanoparticles in quasicrystalline matrices, was studied. Sharply faceted and coherent interfaces can be related to sharper melting transitions, while irregularly shaped and incoherent interfaces can be directly correlated with lowering of melting temperatures. It is shown here that solid lead forms a high energy interface with phason strain-free quasicrystal (resulting in a lowering of the melting temperature) while bismuth forms a low energy interface with the quasicrystal (resulting in superheating, unusual for bismuth).

Keywords. Nanomaterials; nanocomposites; interface; melting; quasicrystal.

1. Introduction

Nanotechnology is beginning to play a major role in our lives to bring us the ultimate in miniaturisation. Many properties and much of the working of devices of nanosized materials will depend on the characteristics of the interfaces in them. It must, therefore, be understood how size in the nano range affects the stability of materials. In particular, what role the structure of the interfaces plays in it.

Gibbs free energy G of solid and liquid phases may be written as:

$$G_s = \nu_s(E_s + G_v^s) + A_s\sigma_s \tag{1}$$

and

$$G_1 = \nu_1(E_s + G_v^1) + A_1\sigma_1, \tag{2}$$

where the subscripts and superscripts s and l refer to solid and liquid phases respectively, ν and A are the volume and area of the particle, G_v is the free energy per unit volume in the

bulk phase, E is the average strain energy, and σ is the surface energy per unit area. Melting occurs by a change in the Gibb's free energy,

$$\Delta G = 4\pi r^2(\sigma_l - \sigma_s) + \frac{4}{3}\pi r^3 \left[\frac{L}{T_0}(T_0 - T_m) + \Delta E\right], \tag{3}$$

where ΔE is the change in strain energy density on melting, T_0 is the bulk melting temperature and T_m is the actual melting temperature.

When the particle becomes small, the ratio of its surface to volume becomes large, and hence the surface energy term becomes prominent. For the melting criterion that $\Delta G = 0$, the change in melting temperature

$$\frac{T_m}{T_0} = 1 - \left[3\frac{(\sigma_s - \sigma_l)}{r} - \Delta E\right]/L. \tag{4}$$

In case of free particles, the ΔE term is negligible and a monotectic decrease in the melting temperature is observed with decreasing particle size. This decrease is more prominent in the range of very low sizes, 20 nm or less in diameter.

The first experimental demonstration of the depression of melting temperature of small particles (less than 50 nm) was demonstrated by electron diffraction by Takagi (1954), who studied thin films of tin, lead and bismuth. Substantial decrease in the melting temperature with a decrease in the thickness of films of these metals was observed. Further investigations were carried out in transmission electron microscopes (TEM). The melting has been determined by the disappearance of electron diffraction patterns, and the size of the particles calculated from the electron micrographs. By using this technique, Coombes (1972) has shown that the melting temperature of lead depresses by about 200°C for particles of radius 3 nm.

In case of particles embedded in a matrix, the melting temperatures can differ, due to interplay of surface energy and E terms. The matrix can cause a substantial difference to these two terms. There have been a number of studies on melting of metallic nanoparticles embedded in metallic matrices. The particle-matrix composites are normally composed of two (or more) immiscible metals. The matrix material should have a higher melting temperature than the embedded particles whose melting behaviour is studied. The metal immiscible in the matrix is embedded by such techniques as melt-spinning (droplets of one metal are entrapped into another by rapid quenching) or ion implantation (Southin & Chadwick 1978). This experiment provides a contamination-free experiment for heterogenous nucleation and melting.

A number of melting studies have been reported, such as In particles embedded in Al (Saka *et al* 1988; Sasaki & Saka 1991), Pb in *fcc* Al, Cu and Ni (Goswami & Chattopadhyay 1995), Pb in Al (Grabaek *et al* 1990). Superheating has been related to faceting and consequent low interface energies.

Recently, superheating by about 70°C of silver particles of mean size 30 nm embedded in nickel matrix has been shown by Zhong *et al* (2001). The silver particles exhibit a cube-on-cube orientation relationship with the nickel matrix and are faceted on {111} and {100} low energy interfaces. Melting of lead particles has been studied in different *fcc* matrices of aluminum, copper and nickel matrix by Goswami & Chattopadhyay (1995). A strong influence of the shape of the particles on melting behaviour is observed. The lead particles in aluminum and copper matrices are faceted (on {111} and {100} planes), and a fraction of them

exhibit superheating; while the particles in the nickel matrix are roughened and truncated octahedrons and do not exhibit any superheating.

The melting of cuboctahedron-shaped indium particles embedded in aluminum matrix has been observed *in-situ* in a high-resolution electron microscope by Sasaki & Saka (1991). The particles are faceted on {111} and {100} planes, and the melting always starts at a {100} facet, the less dense plane. The effect of planar orientation on melting is shown by studies on a single crystal of lead (Pluis *et al* 1987). Melting starts first on the low density planes. The (110) surface of lead starts to melt about 40°C below the bulk melting temperature (Frenken & van der Veen 1985).

Effect of amorphous matrices have also been studied. Microcrystals of tin in the size range 10–60 nm were embedded in an amorphous carbon matrix (Allen *et al* 1980). *In-situ* TEM showed superheating by 12°C above melting temperature of free microcrystals. This superheating has shown to be consistent with strain energy. Goswami & Chattopadhyay (1996, 1999) showed an unusual lowering of melting temperature of bismuth nanoparticles embedded in an amorphous Al–Fe–Si alloy. This was explained by formation of domain structures in the particles, whose formation was attributed to the crystallographic constraint of the spherical shape due to the amorphous nature of the matrix. Amorphisation of a part of the bismuth particles was also reported (Goswami & Chattopadhyay 1999).

Earlier studies are on particles and matrices with simple structures, which form coherent and faceted interfaces with each other, and some on the effect of amorphous matrices, which produce round shaped particles and incoherent interfaces. This paper examines the melting behaviour of nanosized metallic particles, especially the role of interfaces on it. Such investigations have been made by creating novel interfaces in nanocomposites. This has been achieved by embedding nanosized metallic particles in a matrix with a very different structure. The structure of the matrix has then been varied by heat treatments, resulting in the change of the interface structure, and its affect on the melting behaviour has been studied by differential scanning calorimetry. To bring out the importance of the effect of interfaces, we studied lead nanoparticles embedded in Al–Cu–V amorphous (Singh & Tsai 1999b, 2000), Al–Cu–Fe and Al–Cu–Co quasicrystalline (Singh & Tsai 1998a, 1999a) and bismuth nanoparticles embedded in Al–Cu–Fe quasicrystalline matrices (Singh &Tsai 2001). The matrix phases were varied in the same matrix, keeping all the other conditions the same, and the melting behaviour of the nanoparticles studied. Here we study the effect of various parameters on the melting behaviour of the particles in these matrices.

2. Experimental technique

Alloys of composition $Al_{75}Cu_{15}V_{10}$ and $Al_{65}Cu_{20}Fe_{15}$ were made from high purity metals in an electric arc furnace under argon atmosphere. The Al–Cu–V alloy was remelted with 10 wt% pure lead and melt spun on a copper wheel. Similarly, the Al–Cu–Fe alloy was melt-spun with 10 wt% lead and separately with 10 wt% bismuth.

The lead or bismuth composites in the Al–Cu–V or Al–Cu–Fe matrices were studied with JEOL FX 2000-II, EX 2000-II and EX 4000 transmission electron microscopes, after thinning the melt-spun ribbons by ion-milling.

Melting and solidification behaviour of the embedded lead and bismuth particles was studied in the differential scanning calorimeter (Perkin–Elmer D7). For lead particles, heating runs were made from 50° to 370°C at rate of 10°C/ min, while for bismuth particles, the runs were between 50° and 350°C.

3. Results

3.1 *Melting in amorphous and quasicrystalline matrices: Pb nanoparticles in Al–Cu–V*

The lead nanoparticles had typical sizes of 30 nm in as melt-spun alloy (see figure 1a). A small amount of tetragonal Al_2Cu particles existed, attached to the lead particles. The particles were spherical in shape. Often, these particles were multiply twinned on the {111} planes. Heating runs in the DSC showed that a large fraction of lead particles in this sample melt at 310°C, about 17°C lower than the bulk melting temperature (see figure 2a). On heating to 445·8°C, the matrix transformed to the icosahedral quasicrystalline phase. Figure 1b shows a particle in the quasicrystalline matrix. The particle is multiply twinned.

The sample was heated in the DSC to 450°C to transform the matrix from the amorphous to the icosahedral phase, and then cooled to room temperature. The heating run was then repeated. This time, a large number of the particles melted at about 320°C, about 7°C lower than the bulk melting temperature. The cooling runs did not show any peaks, except a faint exotherm at about 266°C, which shows that solidification of the lead particles occurred over a large temperature range.

3.2 *Quasicrystalline and microcrystalline matrices of Al–Cu–Fe alloy*

3.2a *Melting of lead nano-particles in Al–Cu–Fe matrix:* The size of the embedded nanoparticles was typically 50–70 nm. Particles were faceted on the major symmetry planes of the

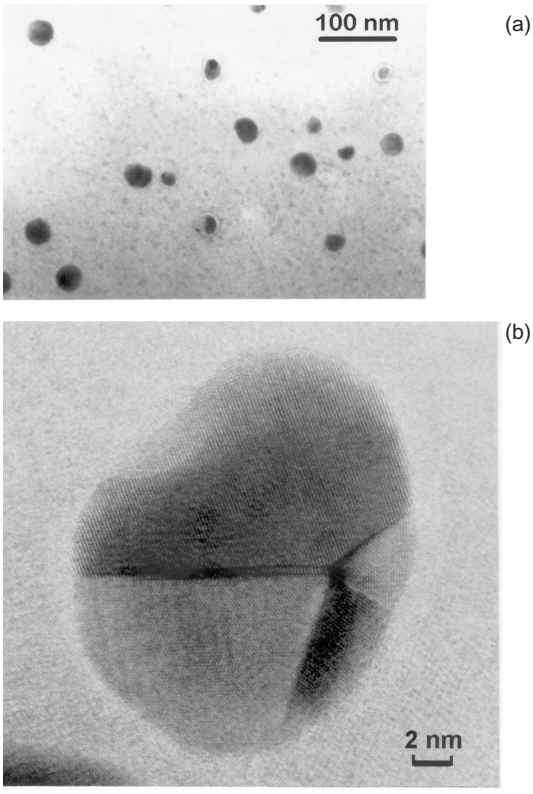

Figure 1. (a) A bright field micrograph showing the distribution of Pb particles in as melt-spun $Al_{75}Cu_{15}V_{10}$ alloy (amorphous matrix). **(b)** A high resolution image of a Pb particle in icosahedral matrix. The particle is multiply twinned. Some facets with the matrix are observed.

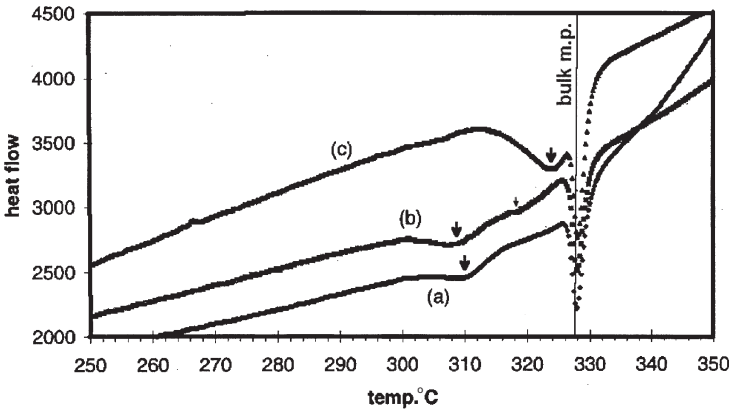

Figure 2. Part of DSC traces for heating runs on the Al–Cu–V samples showing melting of lead in **(a)** amorphous matrix, **(b)** a mixture of amorphous and quasicrystalline matrix and **(c)** quasicrystalline matrix.

matrix icosahedral phase. Tilting experiments in the TEM confirmed that the faceting was on the fivefold, threefold and twofold planes of the icosahedral phase. The two particles seen in figure 3a exhibit twofold and fivefold matrix plane facets. A heavy strain is observed in the matrix.

The samples were annealed at 800°C to remove the strain in the matrix and obtain a perfect icosahedral phase. The effect of annealing was observed as sharp diffraction spots of the icosahedral matrix phase. In the bright field mode, no strain was observed in the matrix. Instead, low-angle boundaries were observed. Figure 3b shows the microstructure after annealing at 800°C. Low angle boundaries are observed, which appear as straight lines passing through the particles. These lines are along the fivefold, threefold and twofold planes.

Another annealing treatment was given at 600°C for 20 h, which is below the stability temperature range of the Al–Cu–Fe icosahedral phase. The diffraction patterns from the matrix showed icosahedral symmetry patterns with broad and multiple peaks. The matrix thus transformed from the icosahedral phase to a multiply twinned microcrystalline state with aggregate icosahedral symmetry. Micrographs after this annealing treatment are shown in figure 3c. After the annealing treatment at 600°C, the lead particles become sharply faceted. These facets are on the pseudo-fivefold, pseudo-threefold and pseudo-twofold planes of the microcrystalline matrix.

Figure 4 shows part of the DSC traces for heating runs on samples that are (a) as melt-spun, (b) annealed at 800°C and (c) annealed at 600°C. In melt-spun samples, particles show melting at the bulk melting temperature. The cooling runs show no peaks, except a few tiny ones corresponding to about 15°C undercooling of lead.

In case of the phason-free icosahedral matrix (the 800°C annealed sample), a lowering of melting temperature by about 6°C is observed. In the sample annealed at 600°C, the Pb particles melt at the bulk melting temperature of 327°C, and exhibit a sharper peak than in case of the melt-spun samples. These samples show absolutely no peaks on cooling.

3.2b *Melting of bismuth nano-particles in Al–Cu–Fe matrix:* In samples containing bismuth particles, the nanoparticles were again about 50 to 70 nm in diameter (see figure 5a). However, in contrast to the case with lead, little or no faceting on the particles was observed. Just as

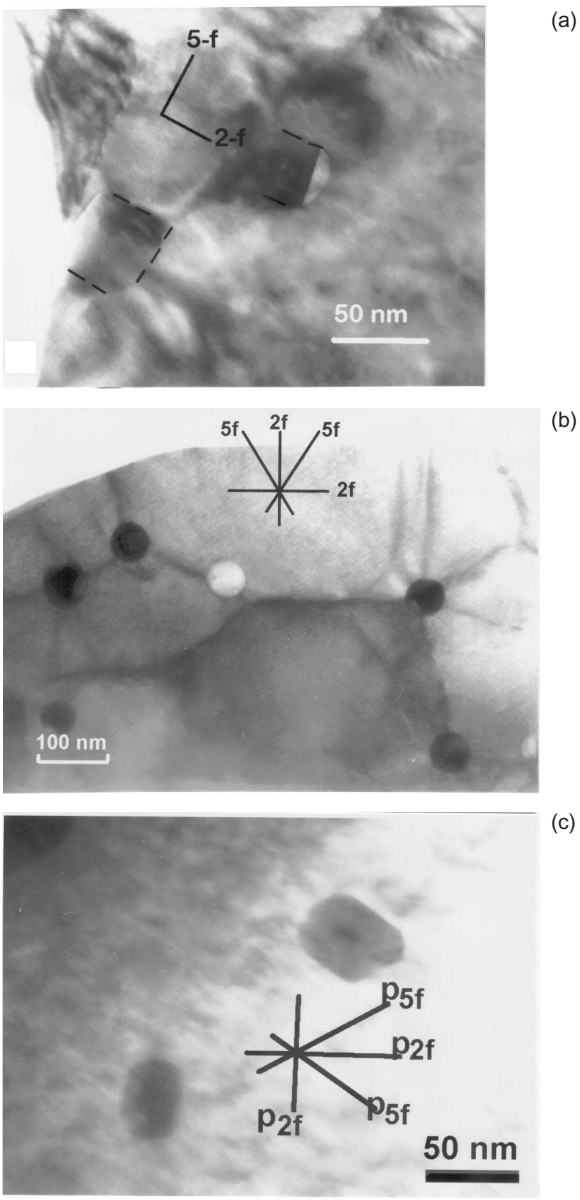

Figure 3. Microstructure of lead particles in $Al_{65}Cu_{20}Fe_{15}$ matrix. **(a)** As melt-spun sample. In this zone axis, twofold and fivefold planes are observed perpendicular to each other, on which facets are observed on the lead particles. A lot of strain is evident in the matrix. **(b)** 800°C annealed sample. This micrograph is in twofold zone axis. The matrix is strain free. Low angle boundaries, on major symmetry planes, run through the particles. **(c)** 600°C annealed sample. The matrix is microcrystalline with aggregate icosahedral symmetry. The micrograph is along a (pseudo) twofold zone axis. Sharp facets on major symmetry planes of the matrix are observed on the particles.

in the case of lead-containing samples, a high density of phason strains was observed in the matrix, as in figure 5a.

Figure 5b shows the microstructure after annealing at 800°C. The phason strains in the matrix are annealed out. Just as in the case of lead-containing samples, low-angle grain boundaries are observed, radiating from the particles. However, these boundaries are not straight but curved. Therefore these lines are not along any preferential direction. Figure 5c shows the microstructure after annealing at 600°C. Contrast due to Moire fringes are observed in the matrix. Slight or no faceting is observed.

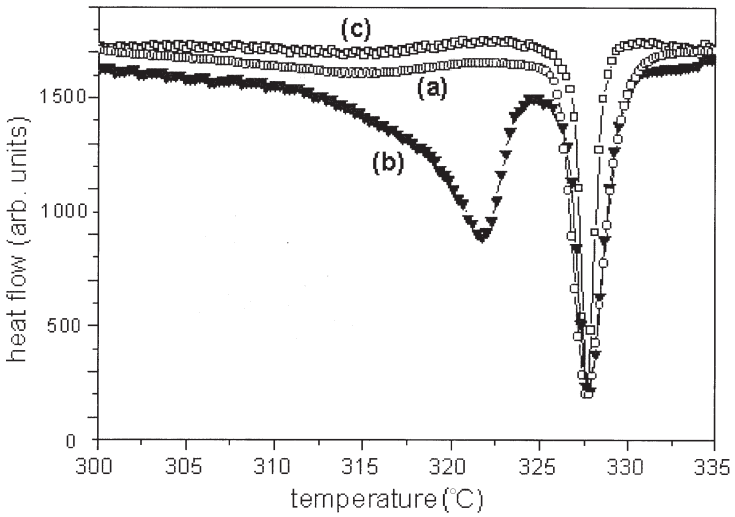

Figure 4. Parts of DSC traces showing melting of lead particles in Al–Cu–Fe matrix in **(a)** the as melt-spun condition, **(b)** annealed at 800°C and **(c)** at 600°C.

Figures 6a and b show high resolution micrographs of particles in 800° and 600°C annealed samples. The micrograph in figure 6a is along a zone axis of icosahedral phase in which a twofold plane is perpendicular to a fivefold plane (these planes are marked in the figure). In this micrograph, a facet is observed on a twofold matrix plane (in other parts of the micrograph, there is an overlap of particle with the matrix). The particle in the 600°C annealed sample (see figure 6b), shows irregular shape and no faceting. No coherency with the matrix is evident.

A part of the DSC traces for heating runs is shown in figure 7. In the as melt-spun samples the bismuth particles show melting at the bulk melting temperature of bismuth. In the 800°C annealed sample also, the bismuth particles melt at the bulk melting temperature. In fact, a fraction of the particles even show superheating, by 7°C. The endotherm at the bulk melting temperature is sharper than that for the as melt-spun sample, and occurs at about 1°C higher than that for the as melt-spun sample. Superheating of bismuth has not been reported in any other matrix. The results seen in the 600°C annealed sample are quite unexpected. A lowering of the melting temperature of bismuth is observed. Some particles start melting about 31°C below the bulk melting temperature. Melting peaks at about 9°C below the bulk melting temperature, and continues up to the bulk melting temperature.

4. Discussion

4.1 *Pressure effects*

Application of pressure can change the melting temperature, given by the Clausius–Clapyron equation,

$$\mathrm{d}p/\mathrm{d}T = L/T_M(V_l - V_s), \tag{5}$$

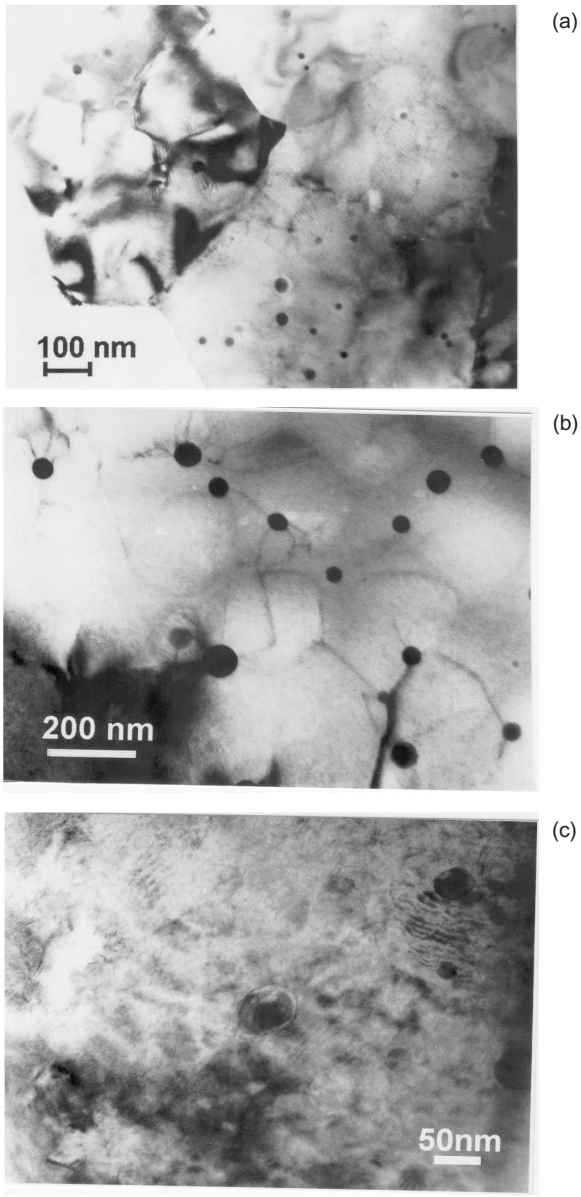

Figure 5. Bright field micrographs of bismuth particles embedded in Al–Cu–Fe matrix. **(a)** As melt-spun sample. Strain in the matrix is evident. **(b)** Annealed at 800°C. Low angle boundaries and dislocations are observed in the matrix. **(c)** Annealed at 600°C. The matrix is microcrystalline.

where L is the latent heat of melting, T_M the melting temperature at atmospheric pressure, and V_l and V_s are molar volumes of liquid and solid phases respectively. In the case of melting under the constraint of a matrix, the source of pressure is the volume change upon melting. Following Roth *et al* (1975), the change in melting temperature ΔT can be given as:

$$\frac{\Delta T}{T_M} = \frac{\delta_f^2}{L}\left[\left(9K + \frac{27EK^2}{8(l+v)\mu^2}\right)/2\left(1 + \frac{3K}{4\mu}\right)^2\right], \tag{6}$$

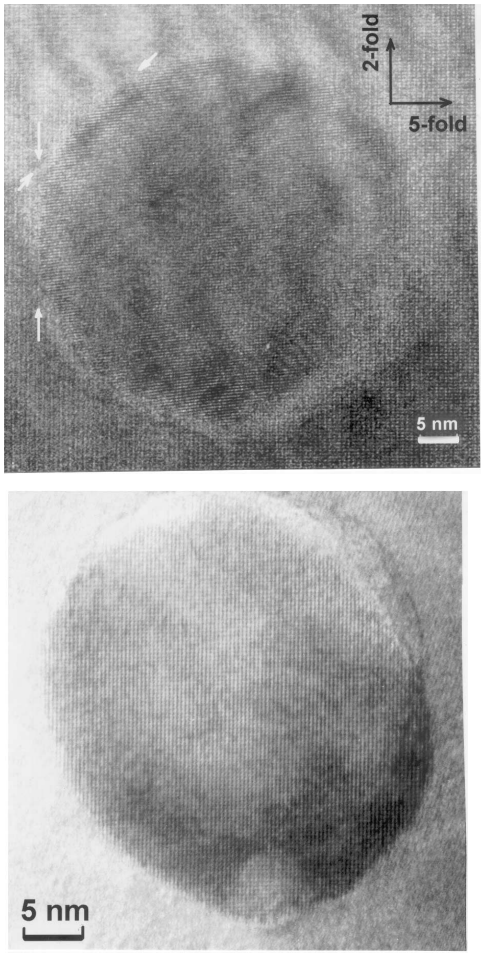

Figure 6. Lattice images of bismuth particles in Al–Cu–Fe matrix. **(a)** Annealed at 800°C. fivefold and twofold planes perpendicular to each other are observed in this zone axis of the matrix. Faceting is observed on the particle (for example, on twofold planes on the left side of the micrograph, marked by arrows). **(b)** In sample annealed at 600°C. No faceting or coherence with the matrix is evident.

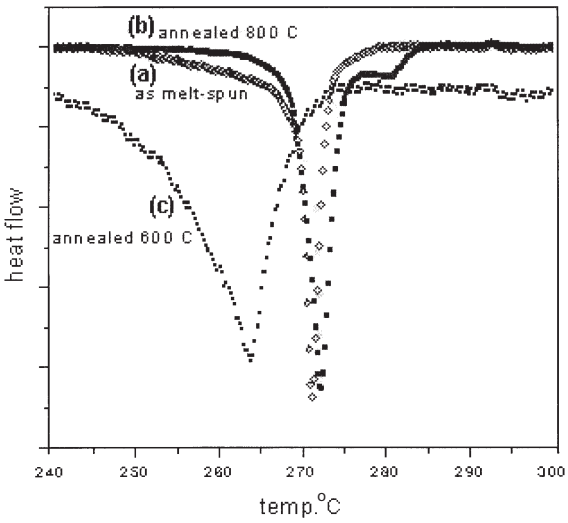

Figure 7. Parts of DSC traces showing the melting of bismuth particles in Al–Cu–Fe matrix in **(a)** as melt-spun sample, **(b)** sample annealed at 800°C and **(c)** at 600°C.

Table 1. Physical properties of lead.

Property	Value	Reference
Bulk melting temperature, T_0	600 K	*Metals handbook* (1990)
Latent heat, L	$2{\cdot}73 \times 10^8$ J/m^3	*Metals handbook* (1990)
Fractional increase in volume upon melting, $3\delta_l$	0·035	*Metals handbook* (1990)
Density solid, ρ_s	11350 kg/m^3	*Metals handbook* (1990)
Density liquid, ρ_l	10680 kg/m^3	*Metals handbook* (1990)
Surface energy solid, σ_s	0·544 J/m^2	Miedema (1978)
Surface energy liquid, σ_l	0·46 J/m^2	Miedema & Boom (1978)
Interface energy, σ_{sl}	0·055 J/m^2	Miedema & Den Broeder (1979)
Thermal exp. coeff. solid, α_s	$29{\cdot}3 \times 10^{-6}$/K	*Metals handbook* (1990)
Thermal exp. coeff. liquid, α_l	$1{\cdot}27 \times 10^{-4}$/K	Faber (1972)
Bulk modulus, K (compressibility)	45 GPa ($2{\cdot}2 \times 10^{-11}$/Pa)	Brandes (1983)

where $3\delta_f$ = unconstrained volume change on melting, K = bulk modulus of the liquid, E = elastic modulus of the matrix, μ = shear modulus of the matrix and ν = Poisson's ratio of the matrix. It is interesting to note that, since δ_f^2 term in this equation is a square, the sign of δ_f is immaterial. The physical constants for lead, bismuth and the Al–Cu–Fe quasicrystal are given in tables 1, 2 and 3 respectively. Plugging in these values for the case of lead embedded in a quasicrystal, $\Delta T/T = 0{\cdot}058$, which gives $\Delta T = 34{\cdot}8^\circ$C. This value can also be compared with that of lead embedded in an aluminum matrix, where $\Delta T = 27^\circ$C (Roth *et al* 1975). The lowering of melting temperature observed in the present study is well within this, and therefore it is possible that it is due to the pressure effect. However, as will

Table 2. Physical properties of bismuth.

Property	Value	Reference
Bulk melting temperature, T	271·5°C	*Brandes* (1983)
Latent heat, L	$5{\cdot}09 \times 10^8$ J/m^3	*Metals handbook* (1990)
Fractional increase in volume upon melting, $3\delta_l$	−0·034	*Metals handbook* (1990)
Density solid, ρ_s	9800 kg/m^3	*Metals handbook* (1990)
Density liquid, ρ_l	1007 kg/m^3	*Metals handbook* (1990)
Surface energy solid, σ_s	0·550 J/m^2	Miedema (1978–79)
Surface energy liquid, σ_l	0·378 J/m^2	*Metals handbook* (1990)
Interface energy, σ_{sl}	0·0544 J/m^2	Turnbull (1950)
Thermal exp. coeff. solid, α_s	$13{\cdot}3 \times 10^{-6}$/K	*Metals handbook* (1990)
Thermal exp. coeff. liquid, α_l	$1{\cdot}1 \times 10^{-4}$/K	Faber (1972)
Bulk modulus K (compressibility)	31·1 GPa ($3{\cdot}21 \times 10^{-11}$/Pa)	Kaye & Laby (1959)

Table 3. Physical properties of icosahedral quasicrystal, Al–Cu–Fe (from Tanaka *et al* 1996).

Property	Value calculated for 623°C from data
Young's modulus, E	112·5 GPa
Poisson's ratio, ν	0·25
Shear modulus, μ	45 GPa

be discussed below, comparison of results of different metals embedded in different matrices in this study leads to the conclusion that it is not the constraint of the matrix, but the particle-matrix interface which is responsible for this.

In the case of bismuth embedded in the Al–Cu–Fe quasicrystal, $\Delta T/T = 0{\cdot}0235$, giving $\Delta T = 12{\cdot}8$°C. The lowering in the melting temperature that is actually observed is in fact more than this calculated value. In the 600°C sample, melting starts 31°C before the bulk melting temperature (the matrix in this case is microcrystalline, but the characteristics of quasicrystal-related crystalline phases are known to be similar to those of quasicrystals). Furthermore, the sign of change in the melting temperature is opposite in the 800°C annealed and the 600°C annealed samples. Thus the pressure effect alone cannot explain the melting phenomenon observed here.

Melting behaviour patterns of lead nanoparticles and bismuth nanoparticles embedded in high perfection icosahedral phase and in microcrystalline aggregates are contrary to that of each other. This can apparently be due to the fact that lead and bismuth have positive and negative volume change respectively, on melting. Thus, if the matrix exerts the same kind of pressure on both, it is expected that the two behave differently. We noted above, however, that the sign of ΔT is independent of the sign of δ. Therefore we will examine the interfaces and show that the melting behaviour can in fact be explained by the interfaces between the particles and the matrix.

The difference in the strain energy density between the solid and the liquid states of the embedded particle, ΔE in (4), is given as (Allen *et al* 1980):

$$\Delta E = \frac{6\mu(\delta_l^2 - \delta_s^2)}{1 + (4\mu/3\,K)}k \tag{7}$$

where $k = a$ constant to account for the effect from the surface of the matrix, and is equal to unity for thick matrices,

$\delta_l =$ misfit parameter for the liquid sphere,

and $\delta_s =$ misfit parameter for the solid sphere.

The $(\delta_l^2 - \delta_s^2)$ term depends on the differential thermal expansion/contraction between the liquid particle and the matrix, and the volume change on melting. The differential radii due to thermal expansion/contraction is given by the term δ_l as:

$$\delta_l = (T_m - T_f)(\alpha_l - \alpha_m), \tag{8}$$

where T_m is the solidification temperature of the matrix (or the annealing temperature of the sample) and T_f is the solidification temperature of the embedded particles), and α_l and α_m are

the linear thermal expansion coefficients for the liquid particle and the matrix respectively. At the freezing temperature, there is a volume change of the particle. This volume change is partly accommodated by the change in volume due to thermal expansion. The term $\delta_l^2 - \delta_s^2$ is given as,

$$\delta_l^2 - \delta_s^2 = 2\delta_l\delta_f - \delta_f^2, \tag{9}$$

where, $3\delta_f$ is as in (6). As can be seen, the sign of δ_f effects this term.

In the present study all samples were formed at higher temperatures. The matrix solidifies first, as the melt cools down. In case of Al–Cu–Fe quasicrystal, this occurs at about 850°C. The matrix and the liquid embedded particles contract as the liquid cools further. Since the thermal expansion coefficient of the quasicrystal is an order of magnitude lower than those of lead and bismuth (tables 1, 2; α_m is assumed to be of the order of 10^{-5}/K for icosahedral quasicrystal (Edagawa *et al* 1998)), the liquid particles contract faster than the matrix, which creates a negative pressure on the particles. This negative pressure delays the solidification in the case of lead (because the solidification involves further contraction) and, in turn, encourages melting on heating from lower temperatures. In the case of bismuth, the melting temperature is actually be expected to be raised. Similar logic also applies to the annealed samples, since annealing temperatures are much higher than the melting/solidification temperatures of the embedded particles.

The actual pressure exerted on the particles is modified by several processes. An annealing treatment, for example, relieves the stress. Grabaek *et al* 1990) observed a pressure on the particles up to 0·16 GPa on gradual heating of the first thermal cycle. Subsequent heating showed no pressure increase. The pressure was estimated by measurement of lattice parameters during *in-situ* high-resolution X-ray diffraction.

Roth *et al* (1975) report an accommodation of the strain on heating by climb of dislocations which existed around the particles in as prepared state. On cooling, a sudden appearance of prismatic dislocation loops punched out of the particles occurred. These processes thus accommodate the strain arising out of volume changes. As we have observed, a high density of phason strain is present in the matrix of the as melt-spun icosahedral phase. On annealing, the phason strain is replaced by low angle boundaries. This process relieves the strain.

In addition to the factors considered above, comparison of results shows that change in the melting temperature can be correlated to change in the interface structure, rather than the particle–matrix material combination, for example, the case of melting in Al–Cu–Fe matrix annealed at 600°C. In this same matrix (crystalline aggregate), bismuth shows a lowering of melting temperature. Considering that the annealing temperature is much above the melting temperature of bismuth, superheating might be expected. The melting temperature also shows a wide scatter in this case. Contrary to this, the lead particles in the matrix of this condition show a very sharp melting peak at the bulk melting temperature, which can be correlated with the emergence of the sharp interfaces with the matrix. We therefore examine the role of interfaces.

4.2 *The role of interfaces*

To bring out the essential differences in the behaviour of lead and bismuth, it will be useful to review their reported behaviour when embedded in simple metal matrices, such as aluminium. Melting of both lead and bismuth particles has been studied in aluminium matrices (tables 4 and 5). While lead is *fcc*, bismuth is rhombohedral. The lead particles in aluminium are faceted, while bismuth in the same matrix shows no facets.

Table 4. Summary of studies on lead particles embedded in aluminum.

Method of preparation	Size of particles	Morphology	Orientation relationship	Super-heating	Reference
Stir and cast in graphite	0·5 μm	Rounded	-	0°C	Roth *et al* (1975)
Ball milling and annealing	13 nm	Irregular	None	−21°C	Sheng *et al* (1998)
Melt-spinning	10 nm	Truncated octahedron	Cube-cube	+103°C	Goswami & Chatto-padhyay (1995)
Ion-implanted / single crystal	14 nm / 27 nm	-	-	+67°C/44°C	Grabaek *et al* (1990)

As has been observed here, the shape of the particles in the as melt-spun samples is dictated by the symmetry of the matrix. In case of the pure metal particles embedded in metallic matrices, on annealing the particle shape changes to that of the intersection point group symmetry of the particle and the matrix. The effect of annealing on particle shape in quasicrystalline matrix has to be considered.

The amorphous matrix imparts a spherical shape to the particles. The particles, however, prefer to solidify with low energy planes on the surface. This is the reason for twinning to occur within the particles. In a constrained volume, twinning can occur to bring the low energy planes to the surface. When the matrix transforms to the quasicrystalline phase, lower energy interfaces between particle and the matrix can occur, as has been observed in case of lead embedded in the Al–Cu–Fe icosahedral phase. AT the temperature at which the

Table 5. Summary of studies on bismuth particles embedded in aluminum.

Method of preparation	Size of particles	Morphology	Orientation relationship	Super-heating	Reference
Stir & cast in graphite	0·5 μm	Faceted?	None	0	Roth *et al* (1975)
Ion-implanted	Few to tens of nm	$\{110\}_{\text{rhomb}}$ facets, otherwise rounded	$\{111\}_{\text{Al}}\|\|$ $\{110\}_{\text{rhomb}}$ (both close packed planes)		Thoft *et al* (1995)
As cast	5–15 μm	Spherical	Only some particles	0	Goswami & Chatto-padhyay (1996)
Melt-spun	20–100 nm	Truncated octahedron {111}&{100} planes of Al	$(111)_{\text{Al}}\|\|$ $(1-102)_{\text{Bi}}$ $[01-1]_{Al}\|\|$ $[20-2-1]^{*}_{\text{Bi}}$	−5	Goswami & Chatto-padhyay (1996)
Ball milling & annealing	22 nm	-	-	−15°C	Sheng *et al* (1998)

*Hexagonal coordinates

transformation of the matrix from amorphous to icosahedral phase occurs, the embedded particles are liquid, and therefore do not constrain the matrix from developing facets. Although not determined experimentally, the lead particles in the Al–Cu–V matrix too should show an orientation relationship with the icosahedral matrix. An indirect confirmation of this is as follows. A large number of lead particles are attached to Al2Cu precipitates, showing a definite orientation relationship (Singh & Tsai 2000). At the same time, the icosahedral phase quite likely nucleates on the Al_2Cu phase when transforming from the amorphous phase. Thus the lead and the icosahedral phase are also orientationally related to each other. Slight facets can be discerned on the particle shown in figure 1b. These facets are on the lattice fringes of the matrix.

The icosahedral matrix imparts a shape bounded by fivefold, threefold and twofold planes to the lead particles. It is quite surprising that in the case of bismuth, the particles in the Al–Cu–Fe icosahedral matrix are non-faceted (in as melt-spun condition). Formation of the facets depends not only for the reason that that these planes are low energy planes of the icosahedral phase, but also as they match with low energy planes of the particles. From the crystallographic studies in the TEM and the high resolution micrographs, it is observed that the low energy plane {111} of the lead particles are in contact with the low energy planes fivefold, threefold and twofold of the icosahedral phase. The atomic configuration on these planes suggest a close atomic matching at such an interface. These interfaces will then be of essentially low energy.

In the case of bismuth, in the absence of such a configuration of low energy planes, formation of facets would not occur. It is observed that when embedded in the crystalline matrix of aluminium, bismuth particles do not show any faceting, except on the {110} planes.

Annealing at 800°C to anneal out the phason strains in the icosahedral matrix results in rounding off of the Pb particles. A change in the shape of the particle occurs towards the shape corresponding to the intersection point symmetry. The change in shape indicates that the interfaces formed on rapid solidification are not stable. The new interface exhibits no coherence with the matrix. The appearance of faceting on bismuth particles after annealing at 800°C is intriguing. Equally intriguing is the absence of faceting in the microcrystalline matrix. This will be discussed below.

In (4), it can be observed that, for a given particle size, the larger the $(\sigma_s - \sigma_l)$ term (i.e., the larger the difference between the surface energies σ_s and σ_l), the larger is the change in melting temperature. In case of embedded particles, σ_s and σ_l terms are replaced by σ_{sm} and σ_{lm}, the interface energies between liquid particle and matrix and solid particle and matrix respectively. When the difference between them is large, a large change in melting temperature occurs.

The σ_{lm} and σ_{sm} terms in the present system are unknown. However, $(\sigma_{sm} - \sigma_{lm})(= \Delta\sigma)$ term can be calculated from (4) and (6). The thermophysical data are taken as in tables 1–3. The linear thermal expansion coefficient of the Al–Cu–Fe icosahedral phase is taken from another icosahedral phase to be $1{\cdot}1 \times 10^{-5}$/K (Edagawa *et al* 1998). Particle size is assumed to be 50 nm. In the case of embedded lead particles, for cooling after annealing at 800°C, the ΔE is about 0·132 GPa. In the case of bismuth particles, the ΔE in 800°C annealed samples is estimated to be about 0·121 GPa, and in 600°C annealed samples about 0·078 GPa.

Using the calculated ΔE (which assumes there are no strain relieving phenomen a in the sample), $\Delta\sigma$ are calculated. In case of the lead containing samples annealed at 800°C, for $\Delta T = 7$°C, $\Delta\sigma = 2{\cdot}26\,\text{J/m}^2$, and for $\Delta T = 16$°C, $\Delta\sigma = 2{\cdot}32\,\text{J/m}^2$. In case of bismuth containing samples annealed at 800°C, for $\Delta T = -7$°C (superheating), $\Delta\sigma =$

$-2{\cdot}12\,\mathrm{J/m^2}$. In case of bismuth containing samples annealed at 600°C, for $\Delta T = 9$°C, $\Delta\sigma = -1{\cdot}16\,\mathrm{J/m^2}$, and for $\Delta T = 31$°C, $\Delta\sigma = 0{\cdot}82\,\mathrm{J/m^2}$. To compare with the values for equilibrium with vapour (tables 1 and 2), $\Delta\sigma$ for lead and bismuth are $0{\cdot}084\,\mathrm{J/m^2}$ and $0{\cdot}172\,\mathrm{J/m^2}$ respectively. The calculated values for the embedded metals in quasicrystal matrix are not only large, but also have the same sign for both superheating and lowering of the melting temperature.

The $\Delta\sigma$ are calculated again assuming no strain because of the matrix. In case of lead, for $\Delta T = 7$°C and 16°C, $\Delta\sigma = 0{\cdot}053$ and $0{\cdot}121\,\mathrm{J/m^2}$ respectively. In the case of bismuth, for $\Delta T = -7$°C (superheating), 9°C and 31°C, the $\Delta\sigma$ are $-0{\cdot}11, 0{\cdot}14$ and $0{\cdot}72\,\mathrm{J/m^2}$ respectively. Thus in the case of bismuth embedded in a quasicrystalline matrix,

$$\sigma_{sm} < \sigma_{lm}.$$

In the matrices studied here, the difference between the atomic structure of the particles and of the matrices are very large. This can result in large interfacial energy, even when a good atomic match occurs at the interface. On the other hand, liquids and amorphous phases are believed to contain icosahedral clusters (Frank 1950). It can particularly be inferred in case of Al–Cu–V that the structures of the amorphous phase and the icosahedral phase have similar structural units, because the interfacial energy between these two phases is estimated to be very small, of the order of $0{\cdot}002\,\mathrm{J/m^2}$ (Holzer & Kelton 1991). Therefore the interfacial energy between liquid metals and amorphous/quasicrystalline matrices can be small, resulting in a lowering of the melting temperature.

Orientation relationships determined in case of the lead particles embedded in the icosahedral Al–Cu–Fe alloy (Singh & Tsai 1998b, 1999a) suggest that a local atomic match at the interface is favoured. Faceting makes it possible to have coherent interfaces. In case of the icosahedral matrix, a strictly coherent matrix is not possible, because one of the phases is quasicrystalline. However, a good atomic match at the interface, provided by definite orientation relationships leads to low energy interfaces. Such lattice matches are evident in the lattice images from the TEM. When the matrix is in the microcrystalline state, in the case of lead in Al–Cu–Fe matrix, the coherence across the interface with lead is excellent, and the interfaces are sharp and straight.

The properties of bismuth are unusual, in that in solid form it makes relatively low energy interfaces with the icosahedral phase. When embedded in crystalline matrices, it is known to be the only metallic particle which shows a lowered melting temperature in the aluminium matrix (see a compilation by Andersen *et al* 1995). Hence it is not surprising that it shows a lowered melting temperature in the microcrystalline state of the Al–Cu–Fe matrix. Its ability to form lower energy interfaces with the icosahedral phase is in agreement with its reported tendency to amorphise. Parts of bismuth nanoparticles embedded in Al–Fe–Si matrix are reported to be amorphous (Goswami & Chattopadhyay 1999) and free nanoparticles are reported to be surrounded by an amorphous material (Treilleux *et al* 1993).

5. Conclusions

Melting behaviour of nanoparticles of pure metals lead and bismuth embedded in Al–Cu–V and Al–Cu–Fe alloy matrices has been studied. Embedding was achieved by melt-spinning. The matrix alloys formed amorphous, quasicrystalline and microcrystalline phases, depending upon the condition/heat treatment of the samples. These phases caused special constraints

on the matrix in the form of strain, morphology and novel interfaces. The effect of these constraints on the melting behaviour of the nanoparticles has been studied. It is concluded that:

(1) The matrix of lead particles containing $Al_{75}Cu_{15}V_{10}$ alloy in the as melt-spun condition was amorphous. The embedded lead particles (typical size 30 nm) had spherical shape and often showed multiple twinning. A large fraction of all particles in this matrix melted at about 17°C below the bulk melting temperature of lead.
(2) Al–Cu–V samples were heated to above 450°C to transform the matrix from amorphous to icosahedral quasicrystalline phase. In this matrix the large fraction of lead particles showed melting at about 7°C lower than the bulk melting temperature of lead.
(3) In the melt spun sample of $Al_{65}Cu_{20}Fe_{15}$ alloy containing lead nanoparticles (size about 50 nm) the matrix was quasicrystalline, characterised by a high density of phason strains. The particles showed definite orientation relationship with the matrix, and faceting on major symmetry planes of the matrix. The melting of the embedded lead particles occurred at the bulk melting temperature.
(4) These samples were annealed at 800°C to anneal out the phason strains in the matrix. As a result of this, low angle boundaries formed on the major symmetry planes of the matrix and a rounding of particle shape was observed. A fraction of these lead particles melted at 7°C lower than the bulk melting temperature of lead.
(5) When annealed at 600°C, the matrix became microcrystalline with aggregate icosahedral symmetry. The lead particles developed sharp facets and good coherence across the interface. Lead nanoparticles in this sample showed sharp melting at the bulk melting temperature of lead.
(6) The bismuth-containing Al–Cu–Fe samples also showed an icosahedral matrix characterised by heavy density of phason strain in the as melt-spun condition. The bismuth particles showed little or no faceting, and showed melting at the bulk melting temperature.
(7) In 800°C annealed phason-free matrix samples low angle grain boundaries occurred. The bismuth nanoparticles melted at the bulk melting temperature, a fraction of them even showing superheating by about 7°C. The superheating of embedded bismuth particles is unusual.
(8) In the microcrystalline matrix of 600°C annealed samples, the bismuth particles started melting 31°C below the bulk melting temperature. The embedded particles were irregular in shape, and no coherence at the matrix interface was observed.
(9) A comparison of the results, and calculations based on strain energy calculations show that the change in the melting temperature of the nanoparticles cannot be attributed to strain of the confining matrix. Possibly no strains occur in the annealed samples.
(10) The change in the melting temperature of the particles can be directly correlated to the nature of the particle-matrix interface.
(11) The calculated difference in the interface energies of solid and liquid particles with the matrix (σ_{sm} and σ_{lm}, respectively) is as much as $0{\cdot}121\ J/m^2$ in case of lead particles in phason free icosahedral matrix of Al–Cu–Fe. This energy difference is $-0{\cdot}11\ J/m^2$ in case of bismuth melting in the phason-free icosahedral matrix. This means that the interface energy of liquid bismuth with the icosahedral matrix is higher than the interface energy of solid lead with the same matrix at the bulk melting temperature. In case of bismuth particle melting in the microcrystalline matrix of Al–Cu–Fe, $\sigma_{sm} - \sigma_{lm} = 0{\cdot}72\ J/m^2$ (particle size is assumed to be 50 nm in all cases).

The authors acknowledge all their colleagues for many stimulating discussions.

References*

Allen G L, Gile W W, Jesser W A 1980 The melting temperature of microcrystals embedded in a matrix. *Acta Metall.* 28: 1695

Andersen H H, Johnson E 1995 Structure, morphology and melting hysteresis of ion-implanted nanocrystals. *Nucl. Instrum. Methods Phys. Res.* B106: 480

Brandes E A (ed.) 1983 *Smithells metals reference book* (London: Butterworths)

Coombes C J 1972 The melting of small particles of lead and indium. *J. Phys.* F2: 441

Edagawa K, Kajiyama K, Takeuchi S 1998 Thermal expansion and Gruneisen parameters of quasicrystals. *Mater. Res. Soc. Symp. Proc.*

Faber T E 1972 *Introduction to the theory of liquid metals* (Cambridge: University Press)

Frank F C 1952 Supercooling of liquids. *Proc. R. Soc. London* A215: 43

Frenken J W M, van der Veen J F 1985 Observation of surface melting. *Phys. Rev. Lett.* 54: 134

Goswami R, Chattopadhyay K 1995 The superheating and the crystallography of embedded Pb particles in fcc Al, Cu and Ni matrices. *Acta Metall. Mater.* 43: 2837

Goswami R, Chattopadhyay K 1996a The solidification behaviour of Bi particles embedded in Al matrix. *Acta Mater.* 44: 2421

Goswami R, Chattopadhyay K 1996b Depression of melting point of multidomained bismuth in aliminum based metallic glass of nanocomposites. *Appl. Phys. Lett.* 69: 910

Goswami R, Chattopadhyay K 1999 The melting and solidification of nanoscale Bi embedded in a glassy and crystalline matrix. *Philos. Mag. Lett.* 79: 481

Grabaek L, Bohr J, Johnson E, Johansen A, Sarholt-Kristensen L, Andersen H H 1990 Superheating and supercooling of lead precipitates in aluminum. *Phys. Rev. Lett.* 64: 934

Holzer J C, Kelton K F 1991 Kinetics of the amorphous to icosahedral phase transformation in Al–Cu–V alloys. *Acta Metall. Mater.* 39: 1833

Kay G W C, Laby T H 1959 *Physical and chemistry constants* (London: Longmans)

Metals handbook 1990 Properties and selection: Non-ferrous alloys and special purpose materials. 10th edn. (Am. Soc. Met.) vol. 2, p. 1130

Miedema A R 1978 Surface energies of solid metals. *Z. Metallkd.* 69: 287

Miedema A R 1978–79 The atom as a metallurgical building block. *Philos. Tech. Rev.* 38: 257

Miedema A R, Boom R 1978 Surface tension and electron density of pure liquid metals. *Z. Metallkd.* 69: 183

Miedema A R, Den Broeder F J A 1979 On the interfacial energy in solid-liquid and solid-solid metal combinations. *Z. Metallkd.* 70: 14

Moore K I, Zhang D L, Cantor B 1990 Solidification of Pb particles embedded in Al. *Acta Mater.* 38: 1327

Pluis B, van der Gon A W D, Frenken J W M, van der Veen J F 1987 Crystal face dependence of surface melting. *Phys. Rev. Lett.* 59: 2678

Roth M, Weatherly G C, Miller W A 1975 On superheating and supercooling of lead and bismuth inclusions in aluminum. *Can. Metal. Q.* 14: 287

Saka H, Nishikawa Y, Imura T 1988 Melting temperature of In particles embedded in an Al matrix. *Philos. Mag.* A57: 895

Sasaki K, Saka H 1991 *In situ* high-resolution electron microscopy observation of the melting process of In particles embedded in an Al matrix. *Philos. Mag.* A63: 1207

Sheng H W, Lu K, Ma E 1998 Melting and freezing behaviour of embedded nanoparticles in ball-milled Al-10wt% M (M = In, Sn, Bi, Cd, Pb) mixtures. *Acta Mater.* 46: 5195

*References in this list are not in journal format

Singh A, Tsai A P 1998a Heterogeneous nucleation of lead on quasicrystals. *Philos. Mag. Lett.* 77: 89
Singh A, Tsai A P 1998b Crystallography and solidification behaviour of nanometric Pb particles embedded in icosahedral and decagonal quasicrystalline matrix. *Acta Mater.* 46: 4641
Singh A, Tsai A P 1999a Stablility on interface between lead particles and quasicrystals and its effect on the melting temperature of the lead particles. *Philos. Mag. Lett.* 79: 561
Singh A, Tsai A P 1999b Melting temperature of lead nanoparticles embedded in Al–Cu–V amorphous and quasicrystalline matrices. *Proc. Int. Conf. Solid-Solid Phase Trans. '99* (JIMIC-3) (eds) Koiwa M, Otsuka K, Miyazaki T (The Japan Institute of Metals) p. 1353
Singh A, Tsai A P 2000 Melting and solidification behaviour of lead nanoparticles emebdded in amorphous and quasicrystalline matrices of Al–Cu–V. *Jap. J. Appl. Phys.* 39: 4082
Singh A, Tsai A P 2001 Melting behaviour of bismuth nanoparticles embedded in Al–Cu–Fe quasicrystalline matrix. *Scr. Mater.* 44: 2005
Southin R T, Chadwick G A 1978 Heterogenous nucleation in solidifying metals. *Acta Metall.* 26: 223
Takagi M J 1954 Electron diffraction study of liquid-solid transition of thin metal films. *Phys. Soc. Jap.* 9: 359
Tanaka K, Mitarai Y, Koiwa M 1996 Elastic constants of Al-based icosahedral quasicrystals. *Philos. Mag.* A73: 1715
Thoft N B, Bohr J, Buras B, Johnson E, Johansen E, Andersen H H, Sarholt-Kristensen L 1995 Melting and solidification of bismuth inclusions in aluminium. *J. Phys.* D28: 539
Treilleux M, Fuchs G, Montandon C, Santos Aires F, Melinon P, Cabaud B, Hoareau A 1993 Atomic rearrangement of supported Bi particles observed by high-resolution electron microscopy. *Philos. Mag.* A67: 1071
Turnbull D 1950 Formation of crystal nuclii in liquid metals. *J. Appl. Phys.* 21: 1022
Zhong J, Zhang L H, Jin Z H, Sui M L, Lu K 2001 Superheating of Ag nanoparticles embedded in Ni matrix. *Acta Mater.* 49: 2897